ACS Photonics

Article

Cite This: ACS Photonics 2018, 5, 1779−1785

Reconfigurable Metagratings

Younes Ra'di[†] and Andrea Alù*[,†,‡,§,⊥]

[†]Department of Electrical and Computer Engineering, The University of Texas at Austin, Austin, Texas 78712, United States
[‡]Photonics Initiative, Advanced Science Research Center, City University of New York, New York 10031, United States
[§]Physics Program, Graduate Center, City University of New York, New York 10016, United States
[⊥]Department of Electrical Engineering, City College of The City University of New York, New York 10031, United States

ABSTRACT: Recently, it was revealed that gradient metasurfaces based on continuous gradients of the local reflection and/or transmission coefficients are fundamentally limited on their overall efficiency in transformation of an impinging wavefront. In addition, due to the fastly varying impedance profile that these surfaces require, they usually need high-resolution fabrication processes. To address these issues, the concept of metagrating was recently put forward, enabling engineered surfaces capable of manipulating light with unitary efficiency. Metagratings are periodic arrays of carefully designed scatterers that, in contrast with conventional metasurfaces, do not need to support a continuous gradient surface impedance, and consequently, are far simpler to fabricate. Building up on this concept, here we explore opportunities to realize reconfigurable multifunctional metagratings. The proposed designs provide a highly efficient reconfigurable platform tuned by electrostatically biasing simply structured graphene sheets, paving the way to a new generation of highly efficient designer surfaces.

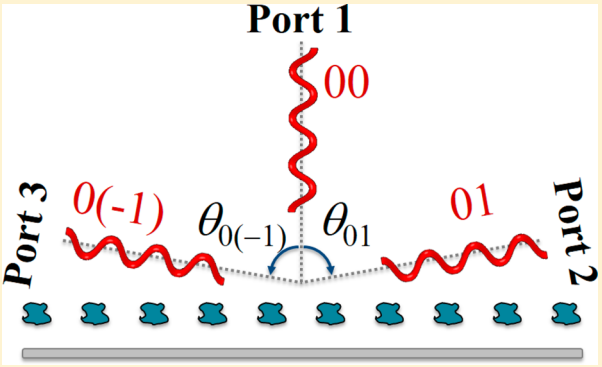

KEYWORDS: *metagrating, metasurface, anomalous reflection, diffraction grating, gradient metasurfaces, graphene*

During the past few years, advances in metasurfaces, two-dimensional arrays of densely located polarizable particles, have led to unprecedented control over the flow of light, enabling several applications in different areas of research and technology, such as energy harvesting, imaging, and cloaking.[1−4] Gradient metasurfaces are an important class of engineered surfaces, which have been widely explored to reroute the direction of incident waves in reflection and transmission.[5−12] These metasurfaces are carefully engineered to provide a gradient surface impedance that enables the required local momentum in order to steer an impinging wave to the desired direction. Although these surfaces have enabled unprecedented functionalities in tailoring electromagnetic waves, a few independent studies have recently proved that gradient metasurfaces, designed based on the generalized laws of reflection and refraction,[5] suffer from fundamental physical bounds on their conversion efficiency,[13−15] as long as they are assumed to be local and passive. Notably, it was shown that active or strongly nonlocal metasurfaces are required in order to reroute an incident wave to a desired direction in reflection with unitary efficiency. In addition, since graded metasurfaces need to provide carefully engineered and fastly varying gradient surface impedance profile, they require high resolution discretization, which results in complications of their fabrication process. Recently, a few approaches were put forward to emulate the nonlocal response required to reroute an incident wave to a desired direction in reflection with unitary efficiency.[16,17] Although these approaches address the inherent limitation of gradient metasurfaces, they still require precise and high-resolution fabrication processes. As a different route, researchers have recently explored the use of adjoint-based optimization methods[18] to find optimal designs based on full optimization of the structures (e.g., see[19]). Although this approach enables designer surfaces that can reroute incident wave with efficiencies higher than conventional gradient metasurfaces, the reported efficiency is typically not unitary. In addition, the surfaces are designed fully based on numerical optimization, without following a systematic and conceptual design route.

In a recent paper, we proposed the concept of metagrating, which enables manipulation of light with unitary efficiency and requires much less fabrication complexity compared to the above-mentioned approaches.[20] This idea has been followed by a few original metagrating designs for efficient electromagnetic wave manipulation in different portions of the electromagnetic spectrum.[21−23] To explain the basic concept underneath the metagrating functionality, let us first consider a conventional flat mirror, for which the reflected wave travels in the specular direction, meaning that incidence and reflection angles are

Special Issue: Ultra-Capacity Metasurfaces with Low Dimension and High Efficiency

Received: December 12, 2017
Published: March 12, 2018

DOI: 10.1021/acsphotonics.7b01528
ACS Photonics 2018, 5, 1779−1785

equal, $\theta_{inc} = \theta_{ref}$. In order to reflect an incident wave to a different direction, the simplest way would be to mechanically rotate the mirror, so as to align the specular direction of the mirror to the desired reflection direction. Graded metasurfaces emulate this mechanical rotation by exploiting a gradient of surface impedance to locally change the reflection phase, which results in bending the direction of the specular reflection. However, the efficiency of gradient metasurfaces designed based on the generalized laws of reflection and refraction cannot be unitary even for small rotation of the specular direction,[13−15] because of the different wave impedance of the impinging and anomalously reflected beams compared to the surface. Metagratings, on the other hand, take a totally different approach to design surfaces capable of rerouting incident waves with unitary efficiency. Instead of adding a transverse momentum to the surface through a gradient of the local reflection coefficient, we set the periodicity so as to align the direction of one of the propagating higher-order Floquet modes with the desired direction of reflection. Naturally, in this scenario, other propagating Floquet modes may also exist. Next, we engineer the scatterer in each unit cell of the metagrating so that its radiation field has nulls in the direction of all propagating Floquet modes other than the one that is aligned with the desired direction of reflection. It was recently shown that this concept can provide extreme wave manipulation with unitary efficiency.[20] Moreover, since metagratings do not need to provide a gradient impedance profile in order to reroute the incident wave, their realization is significantly simpler in comparison to graded metasurfaces.

It should be noted that the concept of metagratings is fundamentally different than the one of conventional gratings and phased array antennas. In the case of conventional gratings,[24,25] the building blocks typically scatter symmetrically, resulting in limited functionality. In the case of the phased array antennas,[26] in each unit cell there is a gradient subarray that is designed to bend the reflected wave into the desired direction, resulting in an efficiency challenge similar to gradient metasurfaces. In metagratings, instead, we exploit the physics of gratings and enrich it by considering complex metamaterial scatterers as the elements forming the grating. In contrast to conventional phased array antennas, the building-block scatterer in metagratings is designed so as to create a radiation null in the direction of all propagating Floquet modes, except the desired one.

In our previous study, it was shown that a single bianisotropic particle in each unit cell can be utilized to create the required asymmetric scattering.[20] Later, it was shown that two cylinders with different radiuses can be utilized as building blocks of the metagrating in order to create the required asymmetric response.[23] In this paper, we generalize the previously proposed concepts and propose a design that can provide the same asymmetric scattering in a simpler design using two nonidentical electric dipoles in a unit cell. Furthermore, we apply this simplified design to realize reconfigurable metagratings based on graphene. We show that the proposed structure can provide multiple functionalities by tuning just two bias voltages. The efficiency of the proposed design is only limited by dissipation in graphene.

METAGRATINGS

We start by designing a reflective metagrating composed of a periodic array of scatterers located over a ground plane, which can reroute a normally incident wave to a desired direction with unitary efficiency. Based on the concept presented in ref 20, as a first step, we set the periodicity to align the direction of one of the propagating Floquet modes with the desired direction of reflection. Since the angle of specular direction is fixed, the easiest way would be to align the direction of the 01 or $0(-1)$ modes with the desired reflection direction. We choose to align the $0(-1)$ Floquet mode with the desired reflection direction (i.e., $\theta_{0(-1)} = \theta_{ref}$). The periodicity of the metagrating p can be written in terms of the wavelength λ and the angle of the $0(-1)$ Floquet mode $\theta_{0(-1)}$ as

$$p = \frac{-\lambda}{\sin \theta_{0(-1)}} \tag{1}$$

Diffraction angles are defined here in the clockwise direction with respect to the z-axis (see Figure 1). Next, we need to design the metagrating so as to cancel the fields of all propagating Floquet modes except the $0(-1)$ mode. In principle, it is possible to align any higher order mode (i.e., $0(\pm n)$ modes with $n \geq 2$) to the desired direction of reflection; however, it will make the cancellation of unwanted Floquet channels more challenging, simply because there are more of them. Therefore, we make sure that 00, 01, and $0(-1)$ are the only propagating Floquet modes, meaning that $|k_{y0(\pm 2)}| > k_0$. Combining this condition with eq 1 results in $\theta_{0(-1)} < -30°$, which means that we should not choose a reflection angle with absolute value smaller than 30°. A smaller reflection angle results in having more propagating Floquet channels, and consequently the unit cell complexity may increase. After setting the period, we design the building-block scatterer so that it supports nulls in the direction of all open Floquet channels other than $0(-1)$ channel. As a first step, the building-block scatterer is designed so that radiation into the specular direction is canceled by the direct reflection of the incident field from the ground plane. Next, the scatterer needs to be designed so that its radiation field has a null in the direction of 01 mode. In our recent study, it was shown that such an asymmetric radiation from a single scatterer can be achieved if we use a bianisotropic omega particle.[20] It was also recently shown that the same asymmetric response can be achieved using two asymmetric cylinders as the building block of the metagrating.[23] Here we propose a more practically feasible and less-complicated design that will serve as a platform to design reconfigurable metagratings.

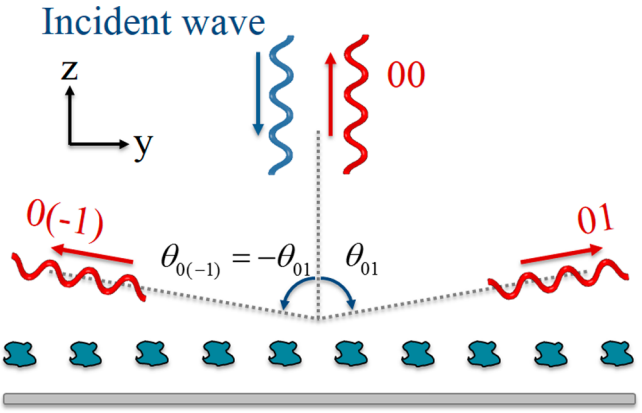

Figure 1. Schematic of a general metagrating with three open Floquet channels.

DOI: 10.1021/acsphotonics.7b01528
ACS Photonics 2018, 5, 1779−1785

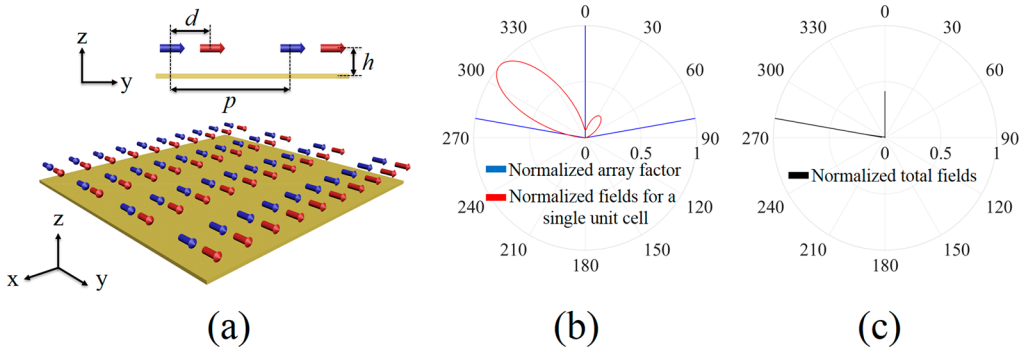

Figure 2. (a) Array of horizontal electrically polarizable particles located over a ground plane. (b) Array factor and radiation field of a single unit cell. (c) Total radiation field.

Figure 2a shows the topology of a metagrating whose unit cell is composed of two nonidentical electric dipoles located over a ground plane. If the metagrating is excited with a normally incident plane wave $\mathbf{E} = \mathbf{y}E_0 \exp(jk_0z)$, the total scattered fields from the array can be written in terms of the Floquet modes

$$\mathbf{E}_{0n} = \left(-\mathbf{y}\frac{k_{z0n}}{k_0} + \mathbf{z}\frac{k_{y0n}}{k_0}\right)\Psi_{0n}\exp(-jk_{y0n}y - jk_{z0n}z),$$
$$\mathbf{H}_{0n} = \mathbf{x}\frac{1}{\eta_0}\Psi_{0n}\exp(-jk_{y0n}y - jk_{z0n}z) \quad (2)$$

where

$$\Psi_{0n} = \frac{j\eta_0}{S}\sin(k_{z0n}h)[I_a^y \exp(-jk_{y0n}d/2) + I_b^y \exp(jk_{y0n}d/2)] \quad (3)$$

Here E_0 is the amplitude of the incident field, k_0 is the free-space wavenumber, $k_{y0n} = 2n\pi/b = k_0 \sin\theta_{0n}$ is the wavenumber in the y-direction, $k_{z0n} = \sqrt{k_0^2 - k_{y0n}^2} = k_0\cos\theta_{0n}$ is the wavenumber in the z-direction, η_0 is free-space wave impedance, $I_{a,b}^y$ is electric current on each dipole, S represents the area of the unit cells, d is the distance between two dipoles in a unit cell, and h is the distance of the array of particles from the ground plane. The specular scattering of the array needs to cancel the direct reflection of the incident field from the ground plane, meaning that $\Psi_{00} + E_0 = 0$. Furthermore, we need to make sure that the array does not scatter into the 01 mode, that is, $\Psi_{01} = 0$. Satisfying these two conditions, we can get the required dipole currents I_a^y and I_b^y as

$$I_a^y = -I_b^y \exp(jk_{y01}d) = \frac{SE_0}{2\eta_0}\frac{\exp(jk_{y01}d/2)}{\sin(k_0h)\sin(k_{y01}d/2)} \quad (4)$$

Here $I_a^y = j\omega\hat{\alpha}_a^{yy}E_{ext}^y$ and $I_b^y = j\omega\hat{\alpha}_b^{yy}E_{ext}^y$, where E_{ext}^y is the impinging electric field in the absence of the array and $\hat{\alpha}_{a,b}^{yy}$ represents the electric polarizabilities of the particles

$$\frac{1}{\hat{\alpha}_a^{yy}} = \frac{-\exp(-jk_{y01}d)}{\hat{\alpha}_b^{yy}} = \frac{-4\omega\eta_0}{S}\sin^2(k_0h)\sin(k_{y01}/2)\exp(-jk_{y01}d/2) \quad (5)$$

The passivity condition requires that the total radiated power carried away from the metasurface through all Floquet modes equals the extinction power

$$\sum_{n=-\infty}^{n=\infty} P_{0n}^z = P_{ext} \quad (6)$$

in the absence of Ohmic losses. The radiated and extinction powers read

$$P_{ext} = \frac{1}{2S}\mathrm{Re}\{\mathbf{J}_e^*\cdot\mathbf{E}_a + \mathbf{J}_m^*\cdot\mathbf{H}_a\},\quad P_{0n}^z = \frac{1}{2\eta_0}\mathrm{Re}\left\{\frac{k_{z0n}}{k_0}\right\}|\Psi_{0n}|^2 \quad (7)$$

In deriving the passivity conditions, we assume that the metasurface sustains only the 0th order mode with respect to the x-axis. This condition should be satisfied independent of the form of the incident wave. For the case under study, only 00 and $0(-1)$ modes are assumed to carry energy. Using eqs 4, 6, and 7, we can get a condition on the distance of the array of particles from the ground plane

$$\sin^2(k_0h)\sin^2\left(k_0\frac{d}{2}\sin\theta_{01}\right) = \cos\theta_{01}\sin^2(k_0h\cos\theta_{01})\sin^2(k_0d\sin\theta_{01}) \quad (8)$$

The metagrating functionality can be explained in terms of antenna theory. Let us assume that we want to design a metagrating to reflect the incident wave to a direction with a reflection angle $\theta_{ref} = \theta_{0(-1)} = -80°$. Knowing the wavelength λ and reflection angle, the periodicity and the distance of the array of particles from the ground plane are set by eqs 1 and 8, respectively. Figure 2b shows the array factor for such an array. (Note that, in this example, the array factor has been calculated for a large aperture size.) This array can, in principle, scatter the incident wave through three open Floquet channels: specular direction with $\theta_{00} = 0°$, the 01 mode with $\theta_{01} = 80°$, and the $0(-1)$ mode with $\theta_{0(-1)} = -80°$. Using eq 4, we can calculate the radiation field of a single unit cell composed of two electric dipoles located over a ground plane. As seen from Figure 2b, the radiation field has a null at the direction of θ_{01}. The total radiation of the array can be calculated by multiplying the array factor with the radiation fields of a single unit cell[27] (see Figure 2c). Therefore, the total field will have a radiation null in the direction θ_{01}. At the same time, the array radiation into the specular direction will be canceled with the direct reflection of the incident field from the ground plane. (Note that, since the polarizabilities derived in eq 5 are the effective ones, the intercoupling effect of the adjacent inclusions has already been incorporated into the polarizabilities of the particles, and consequently, the antenna array analogy is a valid tool to be utilized for studying these structures.)

DOI: 10.1021/acsphotonics.7b01528
ACS Photonics 2018, 5, 1779−1785

Using eqs 2−4, it can be shown that the ratio between the scattered fields into the desired direction (i.e., $E_{0(-1)}$) and into the specular direction (i.e., E_{00}) equals $\frac{|E_{0(-1)}|}{|E_{00}|} = \frac{1}{\sqrt{\cos\theta_{0(-1)}}}$, which guarantees that all the energy received by a unit area of the metagrating will reflect back into the desired direction. It is also worth noting that, in conventional reflectarray antennas, the building block of the array is a graded subarray, designed to locally modify the reflection phase so as to reroute the incident wave to the desired direction in reflection. This approach results in the same efficiency issues as gradient metasurfaces designed based on the generalized law of reflection and refraction.[26] Instead, in metagratings we engineer the scatterer so that its radiation field has zeros at the direction of all Floquet channels except the desired one.

In order to realize the configuration shown in Figure 2a, we can use an array of metallic strips located over a ground plane, as shown in Figure 3a. Before getting into the details of the

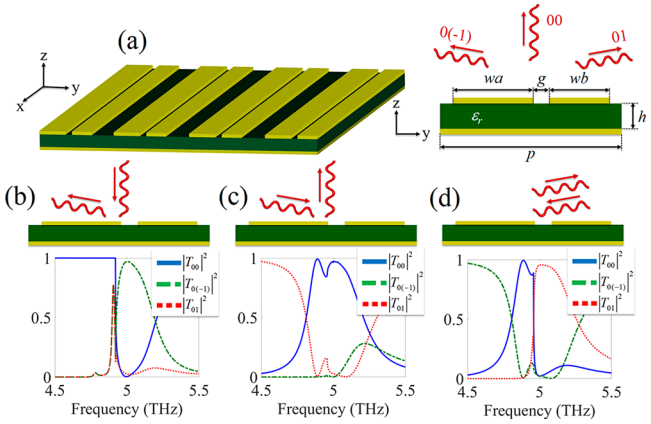

Figure 3. (a) Array of metallic strips located over a ground plane. Scattering results for the case where the structure is excited from the (a) 00 port, (b) 0(−1) port, and (c) 01 port. Design parameters: p = 60.926 μm, h = 0.73 μm, wa = 19.45 μm, wb = 18.5 μm, g = 4.025 μm, and ε_r = 2.2 ($\theta_{00} = 0°$ and $\theta_{01} = -\theta_{0(-1)} = 80°$).

presented designs, it should be noted that all the numerical simulations throughout the paper have been performed using the frequency domain solver of CST Microwave Studio[28] and the design frequency for all the examples presented throughout the paper is 5 THz. We also have assumed that metallic strips and ground plane are perfect electric conductors, therefore the presented designs can ideally scale to the desired frequency of operation by simply scaling the dimensions with respect to the wavelength. Although the presence of loss may naturally decrease the efficiency of the proposed designs, its effect is less strong in comparison to the designs based on other concepts, as investigated in.[21] As it can be seen from Figure 3a, the unit cell of the proposed design is composed of two strips with different widths, whose geometry has been optimized based on the principles outlined in the previous section to provide a null in the direction opposite to the desired one. Note that, in order to design the metagrating, we have simulated the whole array in order to take into account any possible coupling between neighboring particles. The unit cell has been optimized so as to simultaneously achieve the desired scattering characteristics in all open Floquet channels. This metagrating is designed to reroute a normally incident wave to $\theta_{ref} = \theta_{0(-1)} = -80°$. The results shown in Figure 3b indicate that almost 97% of the normally incident power is redirected into the desired direction, that is, $\theta_{ref} = \theta_{0(-1)} = -80$. This structure can be considered a three-port network with 00 (i.e., first port), 01 (i.e., second port), and 0(−1) (i.e., third port) ports. Due to reciprocity, if we excite the structure from the 0(−1) direction (i.e., $\theta_{inc} = \theta_{0(-1)} = -80°$), the incident wave will be fully rerouted to the 00 direction (i.e., $\theta_{ref} = \theta_{00} = 0°$; see Figure 3c). Quite interestingly, followed by energy conservation and reciprocity, if the structure is excited from the 01 direction (i.e., $\theta_{inc} = \theta_{01} = 80°$), the incident wave has to be fully reflected back to the source, meaning that the structure will work as an ideal retro-reflector (see Figure 3d). This retro-reflection feature that is a direct result of energy conservation and reciprocity of the structure may look counterintuitive since specular reflection [i.e., 0(−1) channel for this case] is always an allowed transition, meaning that the specular channel is always open. However, the unit cell does not scatter into this open channel. The corresponding three-port scattering matrix reads:

$$|S| = \begin{bmatrix} 0.06 & 0.15 & 0.99 \\ 0.15 & 0.98 & 0.15 \\ 0.99 & 0.15 & 0.04 \end{bmatrix} \quad (9)$$

Here, ports 1, 2, and 3 correspond to 00, 01, and 0(−1) channels. Note that the two strips used here as the metagrating building block, achieve two parallel goals. First, a periodic array of these unit cells creates a specular radiation that cancels the direct reflection of the incident wave from the ground plane. Second, they support a radiation null in the direction of the 01 Floquet mode when excited from normal incidence. The task of satisfying these two requirements can be made easier if we add one additional strip in each unit cell, providing more degrees of freedom in designing the metagrating. Similar results were independently reported in ref 17, where the proposed structure realizes the nonlocal response required for perfectly rerouting an incident wave into a desired direction, as predicted in refs 13 and 14. However, in comparison to the design in ref 17 that uses up to nine elements in each unit cell, the metagrating presented in this paper is much simpler to design and fabricate, it is based on larger unit elements, and is less prone to loss and absorption.[21]

RECONFIGURABLE METAGRATING BASED ON PATTERNED GRAPHENE

In the previous section, we proposed a practical realization of a metagrating based on purely electric dipoles. Although the proposed concept enables engineered surfaces that can manipulate electromagnetic waves with unitary efficiency, the metagrating functionality is fixed, meaning that as soon as these layers are fabricated, their properties cannot be changed. Here, we explore a reconfigurable metagrating based on the previous concept realized with graphene elements, whose characteristics can be tuned by electrostatically biasing the graphene sheets. Figure 4a represents the proposed structure, whose unit cells are composed of four metallic strips and two graphene sheets controlled through different bias voltages (see Figure 4a). At first glance, the structure looks symmetric, however, the required asymmetry can be achieved by properly tuning the chemical potential of the graphene sheets. Note that, in the case of static design discussed in the previous section, in order to break the symmetry, we use two strips with slightly different width that resonate in two slightly different frequencies. This way, the radiation symmetry of the structure gets broken and

DOI: 10.1021/acsphotonics.7b01528
ACS Photonics 2018, 5, 1779−1785

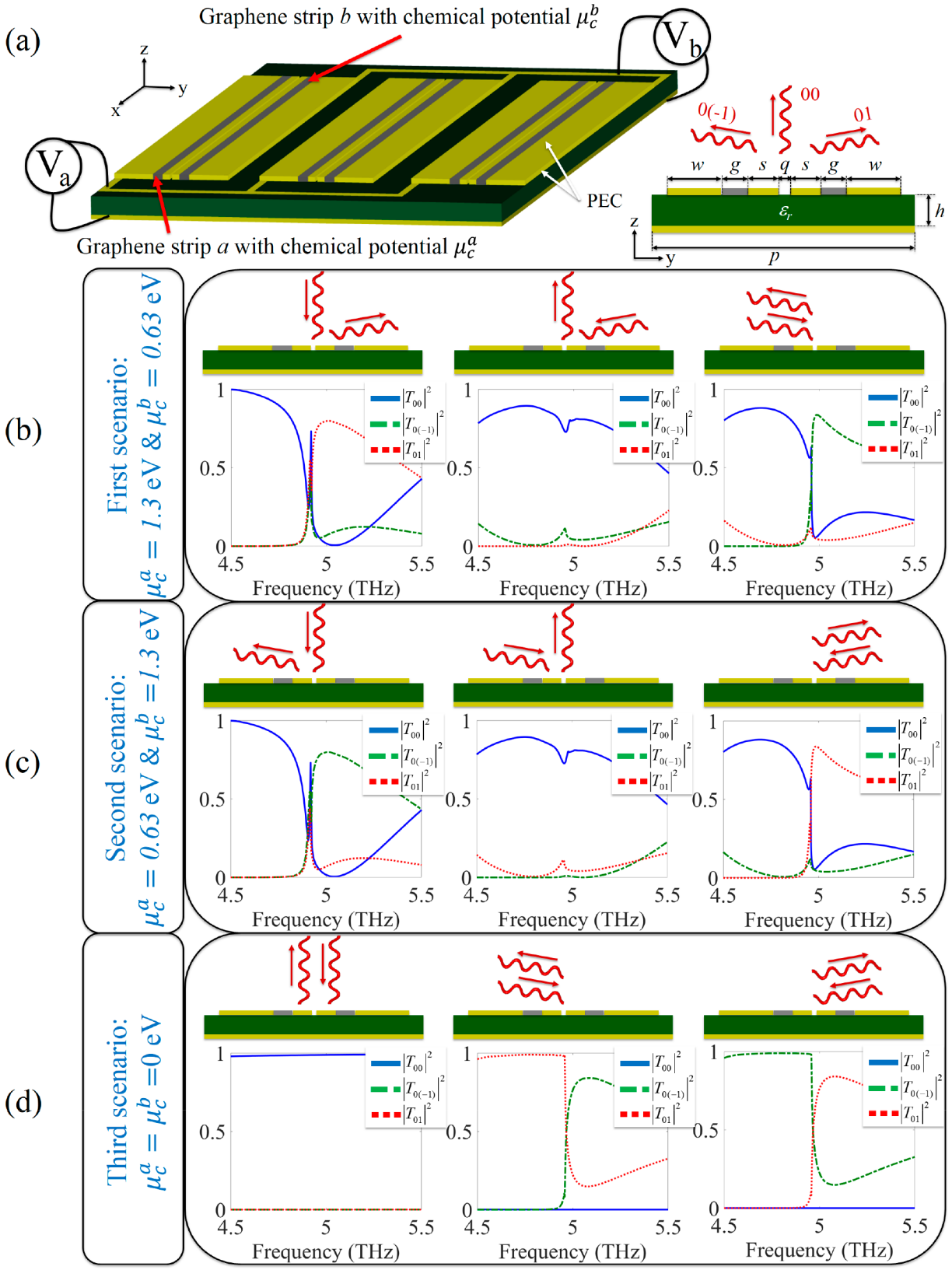

Figure 4. (a) Schematic for a graphene-based reconfigurable metagrating. Results for three different scenarios where (b) μ_c^a = 1.3 eV and μ_c^b = 0.63 eV, (c) μ_c^a = 0.63 eV, and μ_c^b = 1.3 eV, (d) $\mu_c^a = \mu_c^b$ = 0 eV. Design parameters: p = 60.926 μm, w = 19.4 μm, s = 5 μm, g = 2.9 μm, h = 8.5 μm, q = 0.05 μm, and ε_r = 2 (θ_{00} = 0° and $\theta_{01} = -\theta_{0(-1)}$ = 80°). In all simulations we considered τ = 1 ps and T = 300 K. The conductivity values for graphene associated with μ_c = 0 eV, μ_c = 0.63 eV, and μ_c = 1.3 eV are $\sigma_g = 6.5 \times 10^{-5} - j0.1 \times 10^{-3}$ S, $\sigma_g = 7.5 \times 10^{-5} - j2.4 \times 10^{-3}$ S, and $\sigma_g = 15.5 \times 10^{-5} - j4.9 \times 10^{-3}$ S (all values are reported for f = 5 THz), respectively.

DOI: 10.1021/acsphotonics.7b01528
ACS Photonics 2018, 5, 1779−1785

we can create a radiation null in the desired direction. In the case of the reconfigurable design, by changing the chemical potential of the graphene strips, we modify the effective conductivity of the graphene strips and eventually tune two resonance frequencies of the unit cell.

We have found the suitable chemical potential through optimization in CST Microwave Studio.[28] Chemical potentials have been optimized together with other design parameters in order to get any specific design goal. In order to realize the chemical potentials utilized throughout the paper, one can adjust the intrinsic chemical potential of the graphene to a point in the middle of the required range by strong doping of the graphene sheets. Then, by changing the bias voltages, the chemical potentials of the graphene strips can be dynamically tuned to any desired values. Figure 4b shows the results for the case in which the metagrating has been designed so as to reflect a normally incident wave to $\theta_{ref} = \theta_{01} = 80°$. Here, graphene strips have been modeled with infinitesimally thin surfaces characterized with surface conductivity σ_g. This surface conductivity can be expressed using Kubo formalism that relates the surface conductivity of graphene to angular frequency ω, chemical potential μ_c, relaxation time τ, and temperature T as[29]

$$\sigma_g(\omega) = \frac{je^2(\omega - j\tau^{-1})}{\pi\hbar}\left[\frac{1}{(\omega - j\tau^{-1})^2}\int_0^\infty \varepsilon\left(\frac{\partial n_F(\varepsilon)}{\partial\varepsilon} - \frac{\partial n_F(-\varepsilon)}{\partial\varepsilon}\right)d\varepsilon - \int_0^\infty \frac{n_F(-\varepsilon) - n_F(\varepsilon)}{(\omega - j\tau^{-1})^2 - 4\varepsilon^2}d\varepsilon\right] \quad (10)$$

where $n_F(\varepsilon) = (\exp[(\varepsilon - \mu_c)/T] + 1)^{-1}$ is the Fermi distribution function and $\hbar$ is the reduced Planck constant. In this model, we assume that there is no spatial dispersion, whose effects are negligible for the strip size considered here, and that there is no magnetostatic bias. As it can be seen from the left panel in Figure 4b, the incident wave is rerouted toward the desired direction with more than 80% efficiency. We stress that this conversion efficiency includes realistic loss in the graphene sheets, and as such, it is higher than previously proposed reconfigurable gradient metasurfaces based on graphene.[30,31] As seen from the middle panel of Figure 4b, due to reciprocity the same structure will send the wave incident from $\theta_{inc} = \theta_{01} = 80°$ back to a direction normal to the metagrating $\theta_{ref} = 0°$. If the same metagrating is excited from the direction $0(-1)$ with $\theta_{inc} = \theta_{0(-1)} = -80°$, the layer will behave as a retroreflector, sending all the illuminating wave, excluding the dissipated power, back toward the source $\theta_{ref} = -80°$. In this scenario, the metagrating can be seen as a three-port network with the following scattering matrix

$$|S| = \begin{bmatrix} 0.13 & 0.89 & 0.26 \\ 0.89 & 0.07 & 0.21 \\ 0.26 & 0.21 & 0.91 \end{bmatrix} \quad (11)$$

Now we switch the biases for two graphene strips in each unit cell (see Figure 4c). As it can be seen from the left panel of Figure, 4c, in contrast to the first case, the metagrating will reflect normally incident light into the $0(-1)$ mode (i.e., $\theta_{ref} = \theta_{0(-1)} = -80°$). Due to reciprocity, if we excite the layer with an incident wave with $\theta_{inc} = \theta_{0(-1)} = -80°$, the metagrating reflects all the incident wave toward the normal direction (i.e., $\theta_{ref} = 0°$; see the middle panel in Figure 4c). The metagrating will function as a retroreflector if excited through the 01 Floquet channel (see the right panel in Figure 4c). The scattering matrix for this case can be written as

$$|S| = \begin{bmatrix} 0.13 & 0.26 & 0.89 \\ 0.26 & 0.91 & 0.21 \\ 0.89 & 0.21 & 0.07 \end{bmatrix} \quad (12)$$

As a third scenario, we now set the bias voltages of the graphene layers to zero. The left panel of Figure 4d shows that in this case the metagrating works as a conventional reflector when excited with a normally incident plane wave. In addition, if we excite the metagrating from the direction of the 01 or $0(-1)$ modes, part of the power is reflected toward the source and the rest will be transferred into the $0(-1)$ and 01 channels, respectively.

In principle, the metagrating can possibly scatter the normally incident wave into any of these open channels [i.e., 00, 01, and $0(-1)$]. However, in this specific example, that is, when both chemical potentials are zero, the unit cell has two radiation nulls symmetrically located along 01 and $0(-1)$ channels. Therefore, the metagrating has to reflect back all the normally incident wave toward the source. However, when we illuminate this structure from the direction of 01 or $0(-1)$ channels, the illuminated power can be divided between 01 and $0(-1)$ channels. For the specific example under study, most of the illuminated power from 01 or $0(-1)$ channels is reflected back toward the source. Note that, under the consideration of energy conservation, the power division between these two channels can also be engineered by design. The scattering matrix for this case can be written as

$$|S| = \begin{bmatrix} 0.99 & 0.01 & 0.01 \\ 0.01 & 0.87 & 0.47 \\ 0.01 & 0.47 & 0.87 \end{bmatrix} \quad (13)$$

These results indicate that, by just two controlling bias voltages, we can realize a graphene-based reconfigurable metagrating with multiple functionalities tunable in real time. These are just a limited set of functionalities that can be engineered in this structure, but following similar principles we may be able to realize highly efficient reconfigurable metagratings for arbitrary wavefront manipulation.

CONCLUSIONS

In this work, we have extended the metagrating concept, recently introduced to manipulate electromagnetic waves with unitary efficiency and far less complexity in comparison to conventional gradient metasurfaces, to enable reconfigurable metagratings based on graphene strips. In a relatively simple geometry, we have been able to realize at the same time highly efficient deflection of the impinging light to extreme angles in reflection, beyond the efficiency limits of conventional metasurfaces, and to provide a largely reconfigurable response using a quite simple control network. The proposed reconfigurable metagrating can open new research venues in the context of highly efficient wave manipulation using reconfigurable ultrathin devices.

AUTHOR INFORMATION

Corresponding Author

*E-mail: aalu@gc.cuny.edu.

ORCID

Andrea Alù: 0000-0002-4297-5274

DOI: 10.1021/acsphotonics.7b01528
ACS Photonics 2018, 5, 1779−1785

Notes

The authors declare no competing financial interest.

■ ACKNOWLEDGMENTS

We acknowledge the support of the Air Force Office of Scientific Research with MURI grant No. FA9550-17-1-0002, the National Science Foundation, and the Welch Foundation with Grant No. F-1802.

■ REFERENCES

(1) Yu, N.; Capasso, F. Flat optics with designer metasurfaces. *Nat. Mater.* **2014**, *13*, 139−150.
(2) Zhao, Y.; Liu, X.-X.; Alù, A. Recent advances on optical metasurfaces. *J. Opt.* **2014**, *16*, 123001.
(3) Tretyakov, S. A. Metasurfaces for general transformations of electromagnetic fields. *Philos. Trans. R. Soc., A* **2015**, *373*, 20140362.
(4) Glybovski, S. B.; Tretyakov, S. A.; Belov, P. A.; Kivshar, Y. S.; Simovski, C. R. Metasurfaces: From microwaves to visible. *Phys. Rep.* **2016**, *634*, 1−72.
(5) Yu, Na.; Genevet, P.; Kats, M. A.; Aieta, F.; Tetienne, J.-P.; Capasso, F.; Gaburro, Z. Light propagation with phase discontinuities: Generalized laws of reflection and refraction. *Science* **2011**, *334*, 333−337.
(6) Kildishev, A. V.; Boltasseva, A.; Shalaev, V. M. Planar photonics with metasurfaces. *Science* **2013**, *339*, 1232009.
(7) Sun, S.; Yang, K.-Y.; Wang, C.-M.; Juan, T.-K.; Chen, W. T.; Liao, C. Y.; He, Q.; Xiao, S.; Kung, W.-T.; Guo, G.-Y.; Zhou, L.; Tsai, D. P. High-efficiency broadband anomalous reflection by gradient metasurfaces. *Nano Lett.* **2012**, *12*, 6223−6229.
(8) Monticone, F.; Estakhri, N. M.; Alù, A. Full control of nanoscale optical transmission with a composite metascreen. *Phys. Rev. Lett.* **2013**, *110*, 203903.
(9) Esfandyarpour, M.; Garnett, E. C.; Cui, Y.; McGehee, M. D.; Brongersma, M. L. Metamaterial mirrors in optoelectronic devices. *Nat. Nanotechnol.* **2014**, *9*, 542−547.
(10) Kim, M.; Wong, A. M. H.; Eleftheriades, G. V. Optical Huygens metasurfaces with independent control of the magnitude and phase of the local reflection coefficients. *Phys. Rev. X* **2014**, *4*, 041042.
(11) Bomzon, Z.; Biener, G.; Kleiner, V.; Hasman, E. Space-variant Pancharatnam−Berry phase optical elements with computer-generated subwavelength gratings. *Opt. Lett.* **2002**, *27*, 1141−1143.
(12) Asadchy, V. S.; Ra'di, Y.; Vehmas, J.; Tretyakov, S. A. Functional metamirros using bianisotropic elements. *Phys. Rev. Lett.* **2015**, *114*, 095503.
(13) Asadchy, V. S.; Albooyeh, M.; Tcvetkova, S. N.; Díaz-Rubio, A.; Ra'di, Y.; Tretyakov, S. A. Perfect control of reflection and refraction using spatially dispersive metasurfaces. *Phys. Rev. B: Condens. Matter Mater. Phys.* **2016**, *94*, 075142.
(14) Mohammadi Estakhri, N.; Alù, A. Wavefront transformation with gradient metasurfaces. *Phys. Rev. X* **2016**, *6*, 041008.
(15) Epstein, A.; Eleftheriades, G. V. Huygens' metasurfaces via the equivalence principle: Design and applications. *J. Opt. Soc. Am. B* **2016**, *33*, A31−A50.
(16) Epstein, A.; Eleftheriades, G. V. Synthesis of passive lossless metasurfaces using auxiliary fields for reflectionless beam splitting and perfect reflection. *Phys. Rev. Lett.* **2016**, *117*, 256103.
(17) Asadchy, V. S.; Díaz-Rubio, A.; Tcvetkova, S. N.; Kwon, D.-H.; Elsakka, A.; Albooyeh, M.; Tretyakov, S. A. Flat engineered multichannel reflectors. *Phys. Rev. X* **2017**, *7*, 031046.
(18) Bendsoe, M. P.; Sigmund, O. *Topology Optimization: Theory, Methods, and Applications*; Springer: Berlin, Heidelberg, 2003.
(19) Sell, D.; Yang, J.; Doshay, S.; Yang, R.; Fan, J. A. Large-angle, multifunctional metagratings based on freeform multimode geometries. *Nano Lett.* **2017**, *17*, 3752−3757.
(20) Ra'di, Y.; Sounas, D. L.; Alù, A. Metagratings: Beyond the limits of graded metasurfaces for wave front control. *Phys. Rev. Lett.* **2017**, *119*, 067404.
(21) Epstein, A.; Rabinovich, O. Unveiling the properties of metagratings via a detailed analytical model for synthesis and analysis. *Phys. Rev. Appl.* **2017**, *8*, 054037.
(22) Khaidarov, E.; Hao, H.; Paniagua-Domínguez, R.; Yu, Y. F.; Fu, Y. H.; Valuckas, V.; Yap, S. L. K.; Toh, Y. T.; Ng, J. S. K.; Kuznetsov, A. I. Asymmetric nanoantennas for ultrahigh angle broadband visible light bending. *Nano Lett.* **2017**, *17*, 6267−6272.
(23) Chalabi, H.; Ra'di, Y.; Sounas, D. L.; Alù, A. Efficient anomalous reflection through near-field interactions in metasurfaces. *Phys. Rev. B: Condens. Matter Mater. Phys.* **2017**, *96*, 075432.
(24) Silberstein, E.; Lalanne, P.; Hugonin, J.-P.; Cao, Q. Use of grating theories in integrated optics. *J. Opt. Soc. Am. A* **2001**, *18*, 2865−2875.
(25) Tsitsas, N. L.; Valagiannopoulos, C. A. Anomalous reflection of visible light by all-dielectric gradient metasurfaces. *J. Opt. Soc. Am. B* **2017**, *34*, D1−D8.
(26) Headland, D.; Niu, T.; Carrasco, E.; Abbott, D.; Sriram, S.; Bhaskaran, M.; Fumeaux, C.; Withayachumnankul, W. Terahertz reflectarrays and nonuniform metasurfaces. *IEEE J. Sel. Top. Quantum Electron.* **2017**, *23*, 8500918.
(27) Balanis, C. A. *Antenna Theory: Analysis and Design*, 3rd ed.; John Wiley & Sons: Hoboken, NJ, 2005.
(28) CST Studio Suite 2017, http://www.cst.com.
(29) Gusynin, V. P.; Sharapov, S. G.; Carbotte, J. P. Magneto-optical conductivity in graphene. *J. Phys.: Condens. Matter* **2007**, *19*, 026222.
(30) Su, X.; Wei, Z.; Wu, C.; Long, Y.; Li, H. Negative reflection from metal/graphene plasmonic gratings. *Opt. Lett.* **2016**, *41*, 348−351.
(31) Carrasco, E.; Tamagnone, M.; Mosig, J. R.; Low, T.; Perruisseau-Carrier, J. Gate-controlled mid-infrared light bending with aperiodic graphene nanoribbons array. *Nanotechnology* **2015**, *26*, 134002.

DOI: 10.1021/acsphotonics.7b01528
ACS Photonics 2018, 5, 1779−1785